Study of the Fe2CoAl Heusler alloy films growth on the R-plane sapphire substrate by scanning probe microscopy

Article *in* Ferroelectrics · July 2019

DOI: 10.1080/00150193.2019.1574647

3 authors:

Dibya Prakash Rai
Mizoram University
262 PUBLICATIONS **3,085** CITATIONS

SEE PROFILE

Lev Fomin
Russian Academy of Sciences
69 PUBLICATIONS **152** CITATIONS

SEE PROFILE

Gennady M Mikhailov
Russian Academy of Sciences
102 PUBLICATIONS **754** CITATIONS

SEE PROFILE

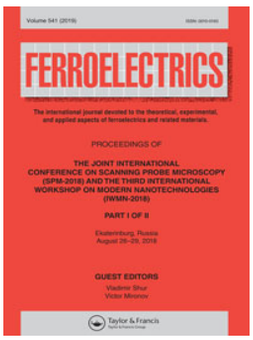

Ferroelectrics

ISSN: 0015-0193 (Print) 1563-5112 (Online) Journal homepage: https://www.tandfonline.com/loi/gfer20

Study of the Fe_2CoAl heusler alloy films growth on the R-plane sapphire substrate by scanning probe microscopy

I. V. Malikov, L. A. Fomin, V. A. Berezin, A. V. Chernykh, D. P. Rai & G. M. Mikhailov

To cite this article: I. V. Malikov, L. A. Fomin, V. A. Berezin, A. V. Chernykh, D. P. Rai & G. M. Mikhailov (2019) Study of the Fe_2CoAl heusler alloy films growth on the R-plane sapphire substrate by scanning probe microscopy, Ferroelectrics, 541:1, 79-92, DOI: 10.1080/00150193.2019.1574647

To link to this article: https://doi.org/10.1080/00150193.2019.1574647

Published online: 09 Jul 2019.

FERROELECTRICS
2019, VOL. 541, 79–92
https://doi.org/10.1080/00150193.2019.1574647

Taylor & Francis
Taylor & Francis Group

Study of the Fe_2CoAl heusler alloy films growth on the R-plane sapphire substrate by scanning probe microscopy

I. V. Malikov[a], L. A. Fomin[a], V. A. Berezin[a], A. V. Chernykh[a], D. P. Rai[b], and G. M. Mikhailov[a]

[a]Institute of Microelectronics Technology and High Purity Materials RAS, Chernogolovka, Russia; [b]Department of Physics, Pachhunga University College, Aizawl, India

ABSTRACT

The grown films of FCA Heusler alloy on the R-plane sapphire with and without the W (001) seed layer were studied using scanning atomic and magnetic force microscopies, supplemented with the results of micromagnetic calculations and measurements of film magnetoresistance. Nonmonotonic dependences of the films' morphological and magnetic properties on their growth temperature caused, as assumed, by the formation of some disordered phase at temperatures of $50 < T_g < 170\,^{\circ}C$ with biaxial magnetic anisotropy were found. A more ordered phase grew in the temperature range $170 < T_g < 400\,^{\circ}C$, in which there was the uniaxial magnetic anisotropy.

ARTICLE HISTORY
Received 29 August 2018
Accepted 26 November 2018

KEYWORDS
Magnetic force microscopy; magnetic anisotropy; magnetoresistance

1. Introduction

Half metal (HM) was first predicted in 1983 [1]. It implies 100% polarization of the conductive electrons spins at the Fermi level, when one of the spin subbands, as an example, is partly occupied in the equilibrium state and the other is not. This makes it possible to reach 100% spin polarized high-density current in such materials.

Attempts to implement HMs by application of binary compounds were not successful enough. Among the materials that have the properties of HM, the most promising are Heusler ternary alloys, which keep being studied intensively. Application of HMs should lead to a significant increase of magnetoresistive effects in devices used in spintronics. Recently, the TMR effect in tens and hundreds of percent at room temperature using monocrystalline epitaxial layers of Heusler alloys has been achieved [2]. For some Heusler alloys, the magnetic anisotropy constants for the films can be significantly lower (by 1–2 orders of magnitude) than for conventional ferromagnets, such as Co or Fe [3]. It allows significant reducing the critical spin-polarized current, which causes the movement of the domain walls in spin transfer torque devices. On the contrary, in other Heusler alloys, anisotropy may be very high, and they can be used as permanent magnets without rare earth elements [4].

For the growth of Heusler alloy films, the method of pulsed laser deposition is widely used, both by simultaneous evaporation from three separate homogeneous targets and

CONTACT L. A. Fomin fomin@iptm.ru
Color versions of one or more of the figures in the article can be found online at www.tandfonline.com/gfer.

by evaporation of one target of the desired stoichiometric composition in high vacuum. Excimer UV lasers or higher harmonics of solid-state Nd: YAG lasers are usually used. Films are grown from a thickness of one atomic layer to 100 nm at temperatures of 20–600 °C on both disordered substrates (e.g. silicon oxide) and monocrystalline substrates (e.g. Si, GaAs [5], MgO, etc.). Grown on ordered substrates, for example, A-plane monocrystalline sapphire Al_2O_3 (11–20) [6], the films exhibit properties close to those of bulk Heusler alloys. R-plane sapphire substrates Al_2O_3 (−1012) that may be used for the growth of epitaxial Heusler alloy films have not previously been applied. However, it may be of interest, since the properties of many materials with a cubic lattice grown on the R-plane sapphire substrate are similar to those grown on the MgO (001) substrate. It should be noted that in epitaxial films of such materials as W, Mo, Nb, Ta, and Fe on the R-plane sapphire, long (including record) residual mean free paths of conductive electrons are achieved [7], which indicates high perfection of the grown films. For many Heusler alloys, the lattice parameter is approximately equal to twice the iron lattice parameter. As it was shown earlier, high-perfect Fe (001) films can be grown on the R-plane sapphire with the Mo or W seed layer [8, 9]. This motivates the study of the Heusler alloys epitaxial films growth on the R-plane sapphire substrate.

The Fe_2CoAl (FCA) Heusler alloy was chosen for experiments. Theoretical consideration of FCA properties [10] shows that its most stable phase is the inverse Heusler structure. The B2 type of the structure is unlikely to be implemented; therefore, the disordered form is the A2 type. In addition, performed calculations have shown that this alloy is not HM [11]. However, it was noted that any deviations, for example, due to non-stoichiometry, the presence of impurities or stresses in the lattice, could lead to the appearance of the HM properties. FCA is a ferromagnet and should have a lattice parameter $a = 0.571$ nm and a Curie temperature of 790 K. The lattice parameter of this Heusler alloy $a = 0.5732$ nm specified in Ref. [12] is almost exactly twice the lattice parameter for iron $a = 0.2866$ nm. The value of the lattice parameter determined in Ref. [13] is only slightly higher and is $a = 0.5766 \pm 0.005$ nm.

Published results of experimental investigations of the properties of the FCA films grown on various substrates are extremely limited. Their magnetic structure is strongly influenced by the often manifested in such alloys uniaxial magnetic anisotropy, which occurs despite the cubic crystallographic symmetry. In this paper, we study how growth conditions, as well as annealing, for the FCA Heusler alloys grown on the R-plane sapphire substrate with and without the W (001) seed layer, affect the morphological and magnetic properties of the studied films.

2. Experimental

The Heusler alloy FCA films with a thickness of 80 nm were grown by pulsed laser deposition using ablation of the FCA target in an ultrahigh basic vacuum 10^{-10} Torr on R-plane monocrystalline sapphire substrates without or with the W (001) seed layer of 10 nm thickness, pre-epitaxially grown at 450 °C. A pulse Q-switch solid-state ($AY:Nd^{+3}$) laser with the wavelength 1.079 mm, 15 ns pulse duration, 20 Hz pulse frequency, and till 0.4 J radiation energy per pulse was used for target ablation.

The FCA films grown at different substrate temperatures, as well as the films subjected to temperature annealing in vacuum at temperatures of 400–700 °C for 1–4 hours, were investigated by atomic force microscopy (AFM) and magnetic force microscopy (MFM), supplemented by magnetoresistance measurements. The film surface was studied by using an AFM P47 Solver (NT-MDT SI) equipped with the tool for measuring magnetic contrast in an external magnetic field.

Based on the results of AFM measurements, the root mean square S_q, of the film surface roughness (defined as the root square of the dispersion) and the correlation length were found from two-dimensional (2d) autocorrelation functions (ACFs) that were numerically built from experimental data of the surface profile after its mathematical processing – subtraction of the base plane and zeroing the mean profile roughness amplitude. A section of the 2d autocorrelation function crossing its main maximum was constructed to determine the correlation length along the film surface arbitrary direction. The full widths of the ACF main peak at half-height in two directions with their maximum and minimum values were considered as the maximum (minimum) correlation lengths L_c.

To measure the magnetoresistance of the grown films, the macrostructures were made in the form of a bridge with lateral dimensions of 200×900 μm^2 by deposition through a mask. The resistance of the bridges was measured using 4-point scheme at room temperature as a function of the external in-plane magnetic field from −1000 to 1000 Oe. The bridge-type structures were oriented with the axis of the bridge along the basic cut (BC) of the R-plane sapphire wafer. The basic cut is defined by the manufacturer ("Monocrystal", Stavropol) as the projection of the C-axis on the R-plane turned counterclockwise by 45 ± 2 degrees. It is noteworthy that the film W (001) or Mo (001) with an axis [100] parallel to the BC [14] is grown on such substrates.

Microstructures in the form of squares and circles were made from the films by subtractive technology, including electron beam lithography, technology of masking coatings, and ion etching [15]. The square microstructures were oriented by their two sides both along the BC or at an angle of 45 to it. The lateral dimensions of microstructures were ranged from 0.5 to 16 μm.

The magnetic states of microstructures were studied by MFM using a two-pass mode (lift mode) similar to that presented in Ref. [16]. The magnetic cantilever oscillated at its resonance frequency. In the second pass, the phase deviation of its oscillations, which is proportional to the second derivative of the magnetic field along the direction perpendicular to the sample surface, was measured. Silicon cantilever (Tipsnano, Moscow) with a resonance frequency of 180 kHz, covered with a layer of iron with a thickness of 50 nm, was used. The magnetic tip was magnetized along its axis. The micromagnetic calculations were used to interpret the magnetic state of microstructures [17], and simulated magnetic contrast was numerically built.

3. Results and discussion

3.1. Surface morphology

Figures 1 and 2 show typical AFM images of the FCA films surface grown at different temperatures on the R-plane sapphire substrate without and with the W (001) seed

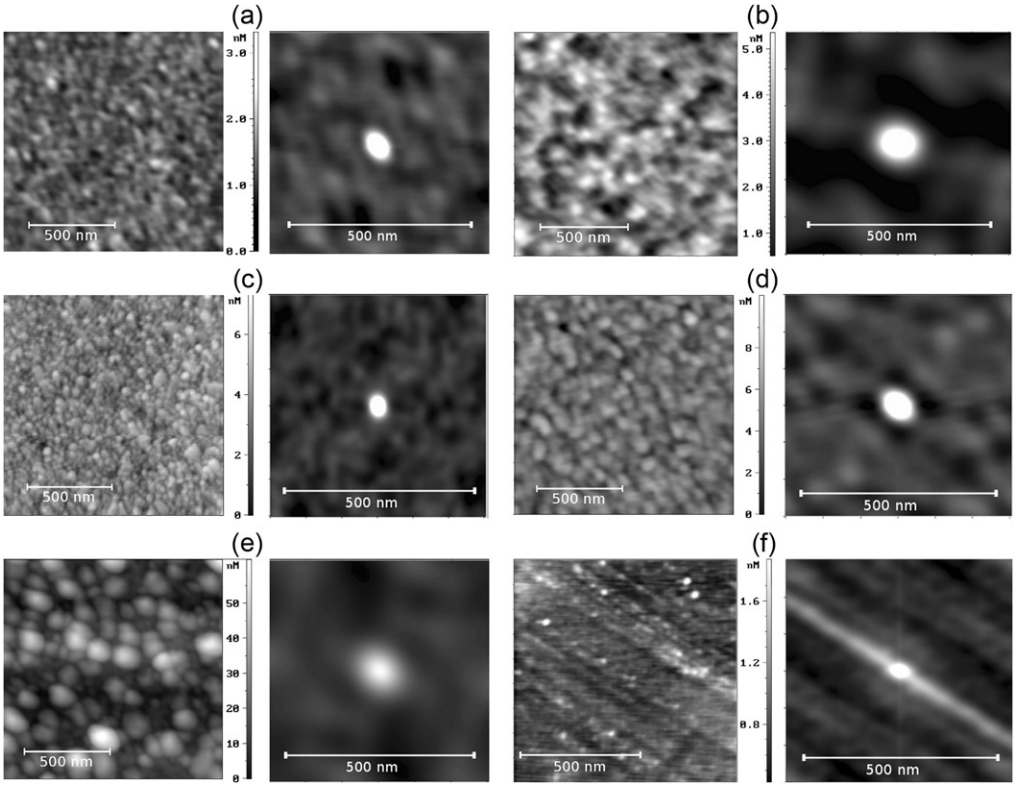

Figure 1. The AFM images of FCA films grown on the R-plane sapphire and their two-dimensional ACFs. Growth temperatures: (a) 20, (b) 200, (c) 280, (d) 420, and (e) 550 °C. (f) The surface profile and ACF for the R-plane sapphire substrate.

layer. X-axes of the AFM scans were parallel to the substrate BC. Numerically built two-dimensional autocorrelations functions are also shown, from which the values of the S_q and the maximum (minimum) correlation length, numerically characterizing the morphology of the surface of the grown films, were found.

The ACFs in these figures have a main peak at their center, characterizing the size of the film crystallites, and also show some structure outside the main peak with a certain symmetry. In most of the ACFs, the main peak is elongated along the direction of about 45° relative to the BC of the sapphire substrate. This direction is close to that of the terraces on the sapphire substrate (Figures 1 and 2f). Such morphological structure of the substrate can influence the appearance of easy axis of magnetization that may be not parallel (or perpendicular) to the BC. For films grown without a seed layer at low (20 °C) and high (550 °C) growth temperatures, the ACFs have the second order symmetry with respect to this axis. However, in the intermediate temperature range the order of their symmetry increases and is close to the fourth one. For films grown with the W (001) seed layer, this behavior cannot be observed, and the ACFs have a symmetry close to the second order everywhere.

The S_q of the grown film roughness, as a function of the film growth temperature, is presented in Figure 3a. At first, the S_q gradually increases from 0.3 to 0.4 nm at T_g = 20 °C to about 1 nm at T_g = 420 °C, and at a further increase, it sharply enlarges to

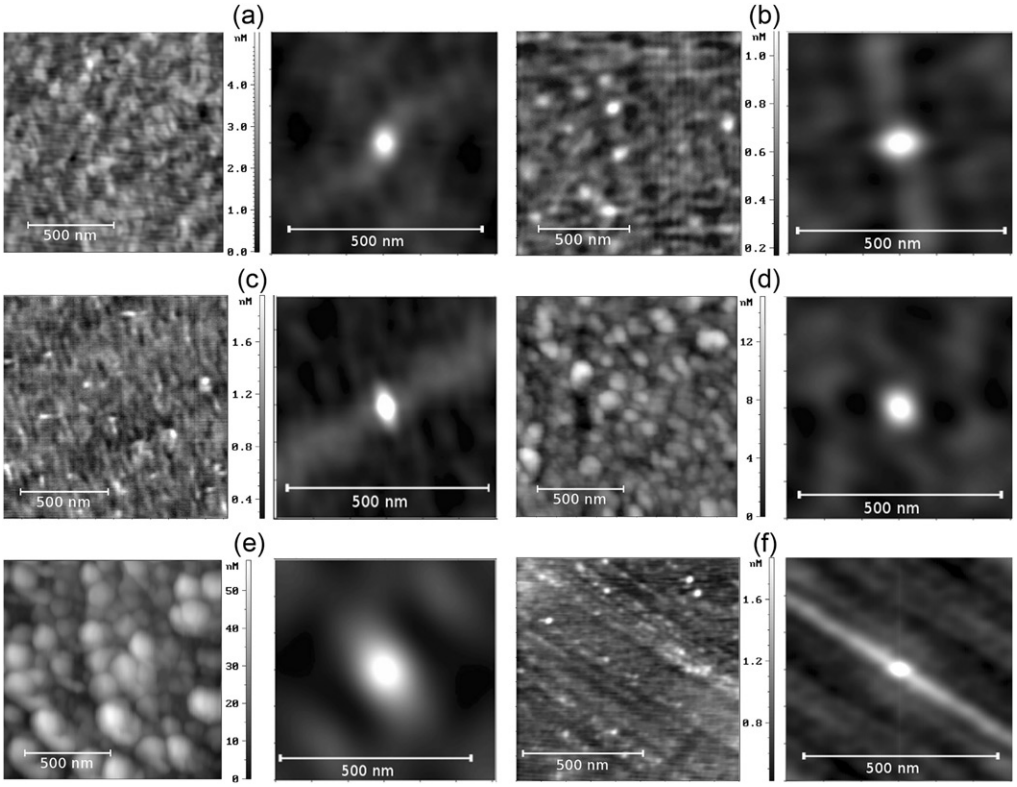

Figure 2. The AFM images of FCA films grown on the R-plane sapphire with the W (001) seed layer and their two-dimensional ACFs. Growth temperatures: (a) 20, (b) 130, (c) 280, (d) 480, and (e) 620 °C. (f) The surface profile and ACF for the R-plane sapphire substrate.

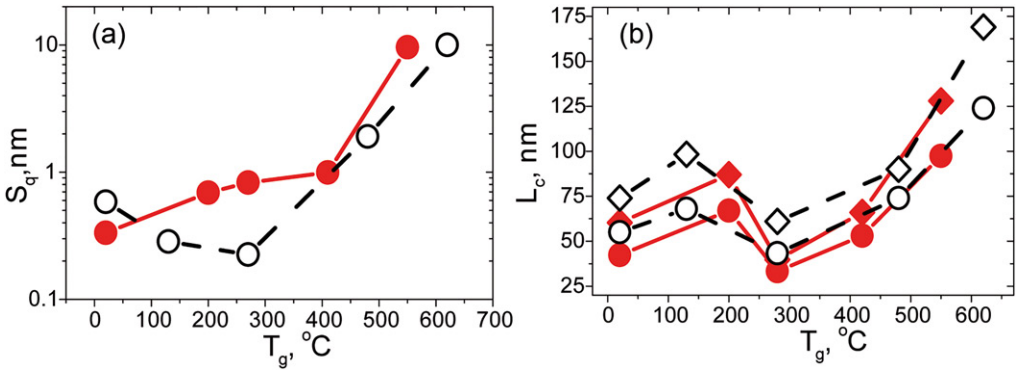

Figure 3. (a) The root mean square S_q of the film surface roughness and (b) correlation length of FCA film surface versus the growth temperature. (a) Full circles indicate data for films grown on the R-plane sapphire, open – for films grown with the W (001) seed layer. (b) Open diamonds and circles show the maximum and minimum values of the correlation length for the films grown on the R-plane sapphire, full diamonds and circles – for the films grown with the W (001) seed layer.

values of more than 10 nm at $T_g = 550$ °C for the films grown on a sapphire substrate. The S_q of the films grown with the W (001) seed layer has a well-defined minimum ($S_q = 0.2$ nm) at a film growth temperature of about 280 °C and also increases sharply at

$T_g > 400\,^{\circ}C$. It should be noted that the similar results on the surface morphology were obtained earlier for iron films grown on the R-plane sapphire with the Mo (001) seed layer. In this case, a minimum of S_q was also observed in the same temperature range, slightly less than 300 °C [9].

At low growth temperatures, the correlation lengths L_c (Figure 3b), found from ACFs (Figures 1 and 2) for both types of samples, increase with the growth temperature, then decrease to the smallest values at $T_g \cong 300\,^{\circ}C$, and then increase again. Such nonmonotonic dependence, as it will be seen further from the studies of magnetoresistance, characterizes phase transformation in the films depending on the growth temperature. Changes in the ratio of maximum and minimum correlation lengths, showing the degree of asymmetry of the main peak of the ACF, are weakly dependent on the film growth temperature. Only for the samples without the W (001) seed layer, the convergence of their values in the temperature region $T_g = 250$–$450\,^{\circ}C$ is observed. Such behavior of this ratio, along with the observed symmetry of the ACF outside the main peak, may be attributed to the influence of the substrate surface morphology.

3.2. The magnetoresistance of the films

The study of the resistance of films versus an external in-plane magnetic field directed parallel or perpendicular to the current in the FCA bridge (longitudinal and transverse magnetoresistance, respectively) also show the dependence of the magnetic properties of the films on their growth temperature. Typical dependences of the resistance versus external magnetic field for FCA films, grown on R-plane sapphire with the W (001) seed layer, are presented in Figure 4 for different growth temperatures T_g. The observed dependences are anisotropic magnetoresistances; the change of the resistance (ΔR) at the coercive field is toward the minimum for longitudinal and maximum for transverse magnetoresistances. Measured dependences of the longitudinal and transverse magnetoresistances (Figure 4a) for the films grown at a low (20 °C) temperatures are rather sharp in their shape and have small both H_c and saturation fields. However, a slight increase in the growth temperature (Figure 4b) up to 70 °C leads to a dramatic change in the form of measured dependences. The magnetoresistance peaks become broad and smooth, the coercive field increases, and the magnetoresistance does not saturate in the fields up to 1000 Oe. With further increase of the growth temperature reaching the growth temperature 280 °C (Figure 4c) the saturation fields and the H_c reduce again to the smallest values $H_c < 10$ Oe. The changes observed at the coercive fields for longitudinal magnetoresistance (ΔR_{long}) become much larger than that for the transverse magnetoresistance (ΔR_{tran}). This indicates the appearance of a uniaxial magnetic anisotropy of such films at this growth temperature with the easy axis of magnetization directed along the bridge and parallel to the BC, if $T_g \cong 300\,^{\circ}C$. With further increase of the growth temperature the coercive field H_c increases again, the peaks of magnetoresistance widen, and magnetoresistance does not reach saturation in the fields up to 1000 Oe.

Based on the results of magnetoresistance measurements, the dependences of the doubled magnitudes of the coercive fields $2H_c$ and the full width of the magnetoresistance peak at half-height ΔH_c were built as functions of the film growth temperature

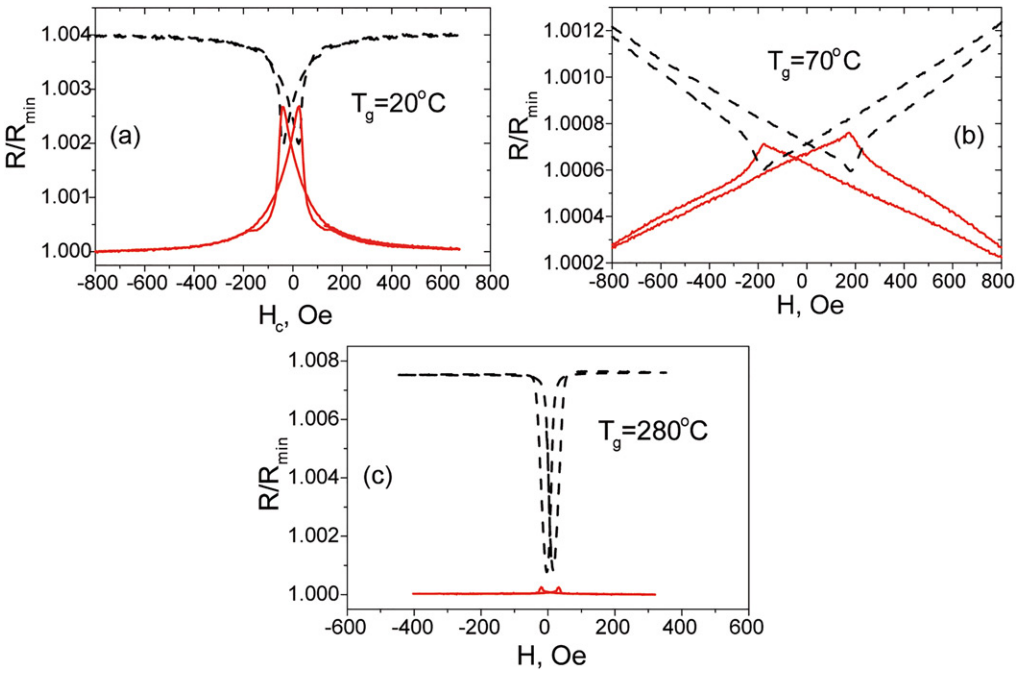

Figure 4. Typical dependences of the longitudinal (dashed line) and transverse (solid line) magnetoresistance of the FCA bridge on the R-plane sapphire with the W (001) seed layer. The films are grown at temperatures of T_g: (a) 20, (b) 70, and (c) 280 °C.

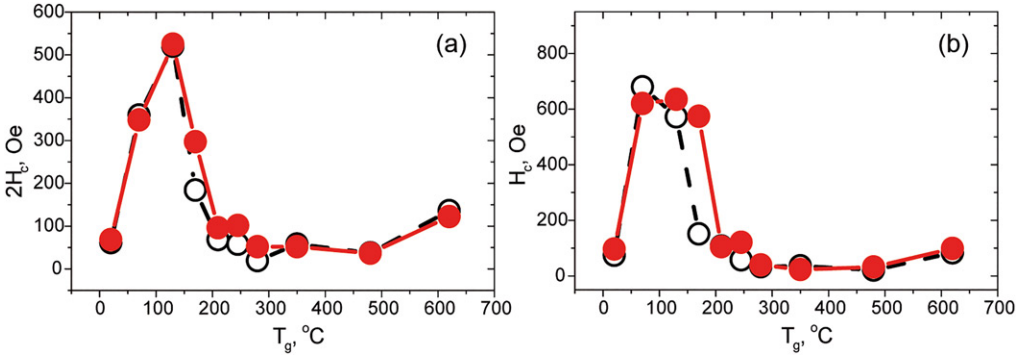

Figure 5. (a) The dependence of the doubled value of the coercive fields and (b) the width of the magnetoresistance peak at half-height in the longitudinal (open circles) and transverse (full circles) magnetoresistances versus the growth temperature for the FCA films on the R-plane sapphire with the W (001) seed layer.

(Figure 5). Films grown at a temperature 20 °C have small values of the H_c and the ΔH_c. With the increase of the growth temperature to 70-150 °C, both values increase sharply by almost an order of magnitude. With a further increase in the film growth temperature till 300 °C, the H_c and ΔH_c reach the minimum value, and the film resistance saturates in the fields of about 100 Oe. The temperature of 280 °C corresponds to the minimum values of the roughness (Figure 3a) and the correlation length (Figure 3b), when using the W (001) seed layer for film growing; analogous minima are

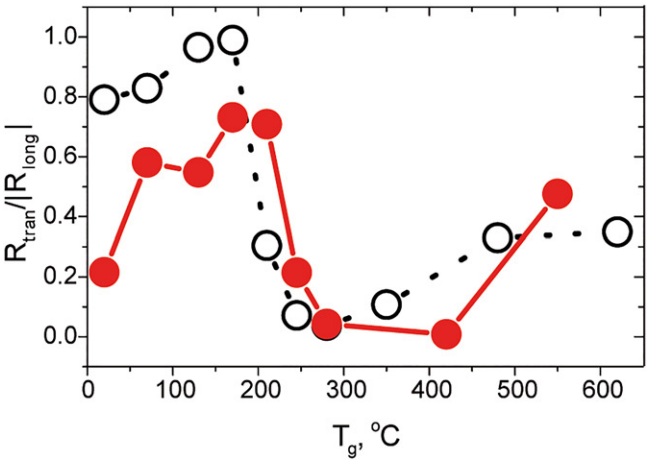

Figure 6. The ratio of the changes in the transverse and longitudinal magnetoresistance at the coercive field H_c as a function of the film growth temperature. Open circles are for films grown with the W (001) seed layer, filled circles – without a seed layer.

observed in the dependence of H_c and ΔH_c (Figure 5). At the elevated film growth temperatures, the values of H_c and ΔH_c increase again. For the films grown on the R-plane sapphire without W (001) seed layer, similar dependences as in Figure 5 were also found.

It should be noted that, despite of the sufficiently close values of the H_c found from longitudinal and transverse magnetoresistances, the changes of their resistances (ΔR) at coercive field can much differ. This indicates the inequity of two mutually perpendicular crystallographic directions. The magnitude of the change in longitudinal magnetoresistance (ΔR_{long}) for bridges grown at approximately 250–400 °C and oriented along the BC exceeds many times that in transverse magnetoresistance (ΔR_{tran}) at the coercive field H_c, although the H_c values for them may only negligibly differ. To demonstrate the effect of magnetic anisotropy, the dependence of the ratio of these amplitudes at the fields of the H_c was depicted in Figure 6. As can be seen from this figure, this ratio at growth temperatures of 70–170 °C for both types of the samples differs from unity not more than in few times, which indicates an approximate equivalence of mutually perpendicular crystallographic directions. On the contrary, at a growth temperature about 300 °C this ratio becomes minimal. As an example, for films grown with the W (001) seed layer, this ratio is equal to 1:23, which proves an appearance of significant magnetic anisotropy demonstrating difference of the magnetic properties with respect to two mutually perpendicular crystallographic directions. Annealing of such films at temperatures up to 600 °C leads to enhancing uniaxial magnetic anisotropy, and the ratio between transverse and longitudinal magnetoresistances ΔR keeps further decreasing.

At a higher film growth temperature $T_g > 400$ °C, the effect of such uniaxial anisotropy weakens. Based on the results obtained, it can be concluded that both uniaxial and biaxial magnetic anisotropy depending on the film growth conditions are observed. For films grown with the W (001) seed layer under optimal conditions at $T_g = 280$ °C, the easy axis of magnetization is directed along the BC. Film annealing at 600 °C for 4 hours leads to an increase in the observed anisotropy effect, which is manifested in almost

complete disappearance of any changes in the experimentally measured transverse magnetoresistance $\Delta R_{tran} \cong 0$ at the coercive field.

These results show that the phase transformations in the FCA films, depending on the growth temperature, are quite elaborate and there is a transition from uniaxial to biaxial (and vice versa) magnetic anisotropy. The observed behavior in the form of non-monotonic dependence in Figure 6 corresponds well to that for the correlation length in Figure 3b. We can assume that in the growth temperature range about T_g = 70–130 °C, there is a phase transform with the growth of some disordered phase, leading to the emergence of a more ordered phase with increasing growth temperature up to T_g = 270–370 °C. With a further increase in the film growth temperature, the ordered phase slowly degrades and biaxial magnetic anisotropy appears.

Comparison of the film properties under the conditions of their growth on the R-plane sapphire with the W (001) seed layer and without it shows that in general they exhibit close dependencies, somewhat differing in details. At the same time, films grown on the R-plane sapphire with the W (001) seed layer under optimal conditions demonstrate higher quality.

3.3. Magnetic state of the films

Microstructures for MFM experiments were fabricated from the films grown at 280 °C with the W (001) seed layer and had the lowest surface roughness and low H_c value. It can be supposed that for the grown films annealed at temperatures till 600 °C, the structural conversion from a disordered to an ordered phase, as a whole, has completed. It follows from the above results of the magnetoresistance study. For comparison, some microstructures are fabricated from the films grown at 170 °C.

MFM images of microstructures made from annealed FCA film grown at 280 °C on the R-plane sapphire with the W (001) seed layer are shown in Figure 7. Microstructures are divided into stripe domains located with their magnetization along the easy axis of magnetization, which is parallel to the BC of the substrate. Triangular closing domains are observed on the ends of the stripe domains. Such domain structure is typical for samples with strong in-plane uniaxial magnetic anisotropy. The shape of the microstructures has less influence on their magnetic state than the crystallographic magnetic anisotropy. The direction of the easy axis of magnetization corresponds to the one previously found from measurements of the magnetoresistance.

However, for microstructures fabricated from FCA on R-plane sapphire with the W (001) seed layer at the growth temperature about 170 °C, which is below the optimum temperature for film growth, it is possible to observe some different picture, when the ordering of the phase is not complete. In these microstructures and bridges that are used for magnetoresistance measuring, the easy axis of magnetization is turned at an angle of 45° to the BC, which may be a manifestation of the substrate surface morphology (Figure 2f). Indeed, the MFM images of microstructures made from the FCA films grown at T_g = 170 °C on the R-plane sapphire with the W (001) seed layer in the form of an 8 × 8 μm^2 square and a circle with a diameter of 8 μm (Figure 8) show uniaxial magnetic anisotropy. In a circular structure (Figure 8b), one can see the central ellipsoidal domain, with the long axis of the ellipse directed at an angle close to 45° to

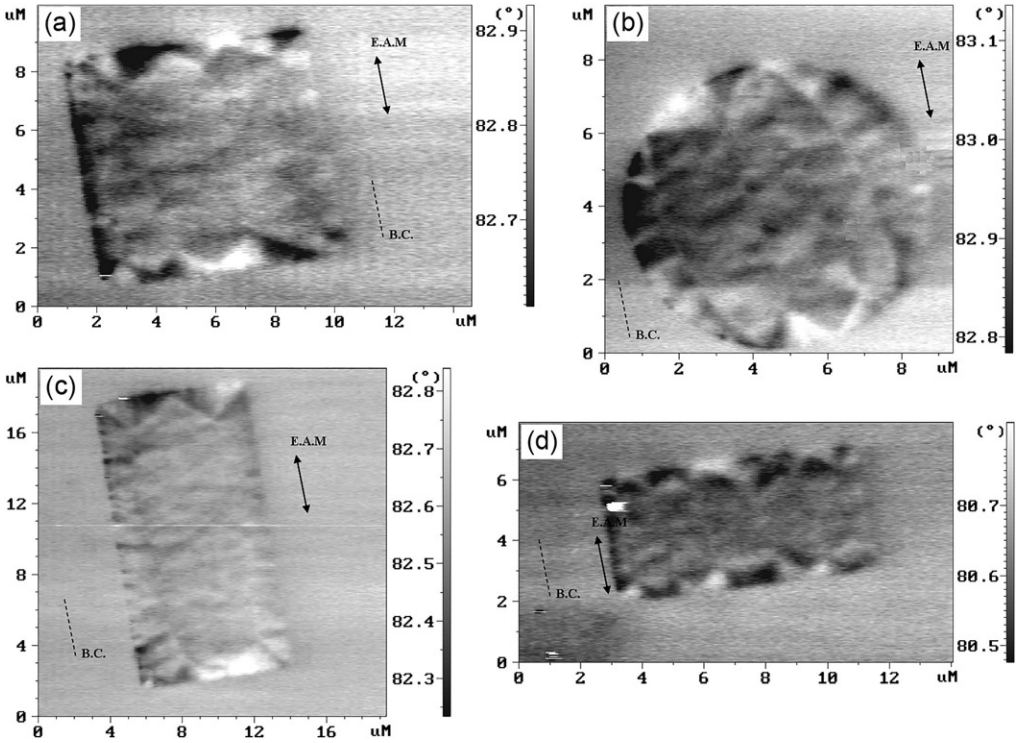

Figure 7. The MFM images of microstructures made from FCA films on the R-plane sapphire with the W (001) seed layer after annealing at 600 °C. The arrows indicate the easy axis of magnetization (E.A.M.), the dashed line – the BC.

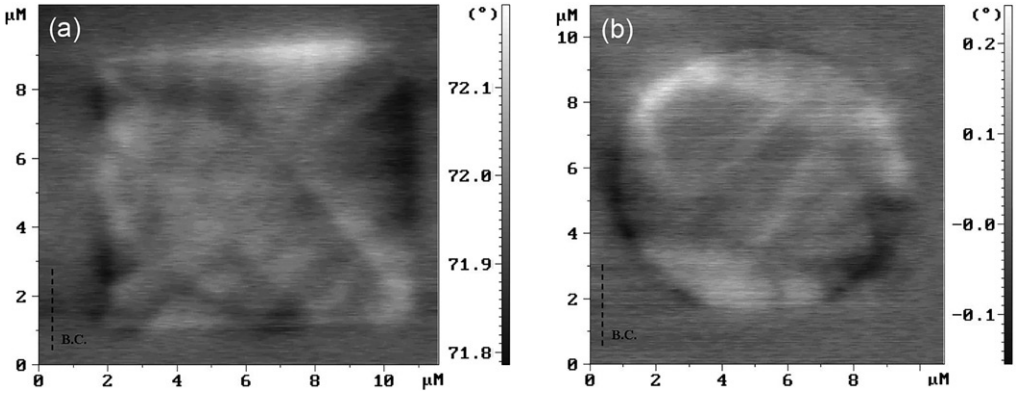

Figure 8. The MFM images of microstructures made from the FCA films grown at $T_g = 170$ °C on the R-plane sapphire with the W (001) seed layer in the form of (a) a 8×8 μm^2 square and (b) a circle with a diameter of 8 μm. The dashed line indicates the BC.

the BC. For the interpretation of the magnetic state, micromagnetic calculations were performed using the OOMMF program [17], and the results of this calculation were used for simulating the magnetic contrast of microstructures. The calculation parameters for the FCA Heusler alloy were obtained from data of Refs. [4, 19]: saturation

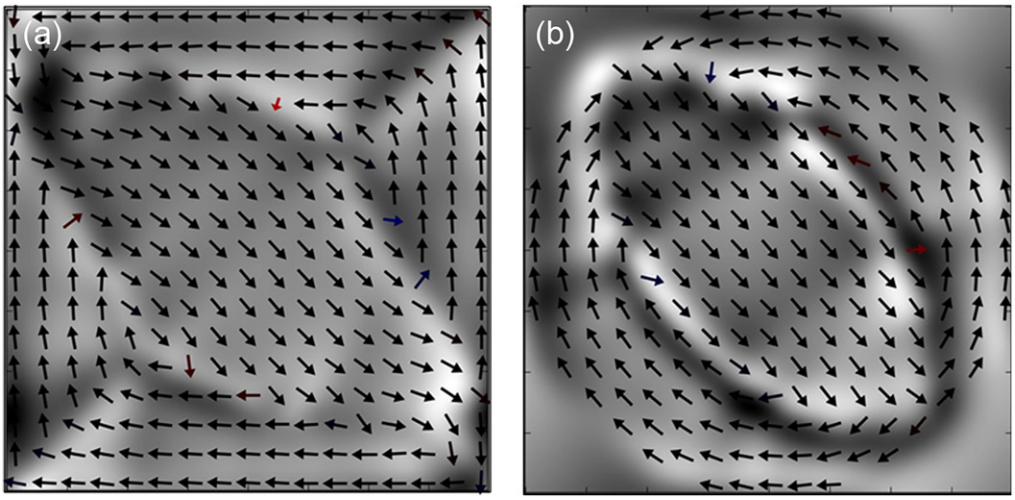

Figure 9. The result of the simulation of MFM images and the calculated magnetization distribution in FCA microstructures in the form of (a) a square and (b) a circle. The image size is 8×8 μm^2. The arrows show the direction of magnetization.

magnetization $M_s = 1043 \times 10^3$ A/m, exchange interaction constant $A = 8 \times 10^{-12}$ J/m, which is almost three times less than that for iron. Data on the anisotropy of this alloy were not known; they generally depend on the type of substrate selected and the quality of epitaxial film growth. For this reason, the anisotropy constant was chosen to obtain the agreement of the simulated magnetic contrast with the experimental MFM measurements. It has been found to be equal to $K = 4 \times 10^3$ J/m^3 that is an order of magnitude smaller than the anisotropy constant of iron. The easy axis of magnetization was set at an angle of 45° to the BC. The size of the calculation cell was $20 \times 20 \times 20$ nm^3. Although this size looks somewhat inflated compared to the commonly used, it still does not exceed the exchange length for this material $l_{ex} = (A/K)^{1/2} \approx 45$ nm. Numerical calculation using the Landau-Lifshitz-Gilbert equation with a large Gilbert damping parameter $\alpha = 0.5$ rapidly converges to a stable magnetic state (Figure 9). It is seen that the calculated MFM contrast is close in main features to the experimental one, although the experimental contrast shows a somewhat more complicated structure.

After annealing microstructures, fabricated from the FCA films grown on the W (001) seed layer, at a temperature of 700 °C, the anisotropy in the film plane changes from uniaxial (Figures 8 and 9) to biaxial one. The magnetic state of the square microstructures was found to be quite complicated. However, the magnetic state of the circle (Figure 10a) is interpreted much more easily. The MFM image of the annealed circular microstructure and its simulation are shown in Figure 10. The magnetic structure in its center represents four mutually perpendicular 90-degree walls mainly of the Neel type. However, small inclination of the magnetization (Figure 10b) out of a circle plane, that is a signature of small admixture of the Bloch type domain wall, is observed. The Neel domain walls are identified by their magnetic contrast, which is light on one side of the wall and dark on the other [18]. The walls divide the circle into four domains, the magnetization of which is directed at an angle of 45° to the domain wall. This magnetic structure is typical for the samples with biaxial magnetic anisotropy in the film plane.

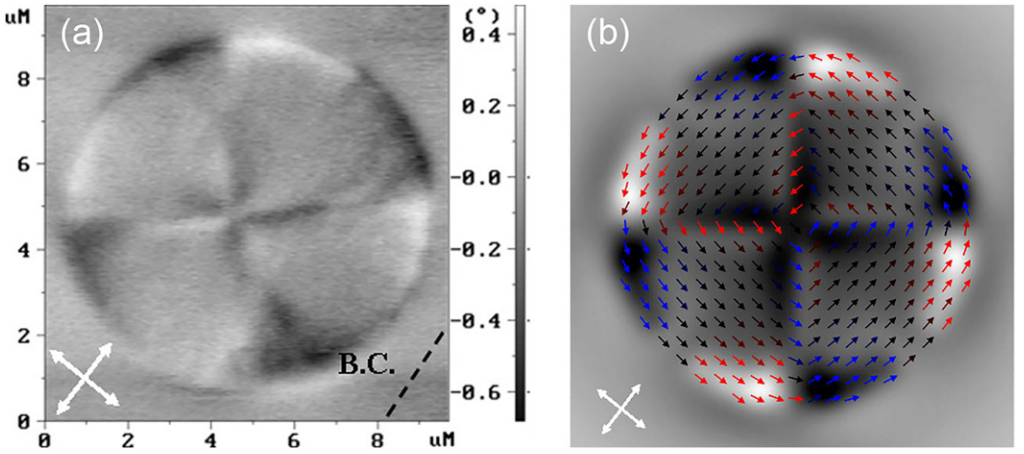

Figure 10. The MFM image of (a) a circular microstructure made from the FCA film after annealing and (b) its simulation. The white arrows indicate the easy axes of magnetization. The black arrows indicate an in-plane magnetization, the red and blue arrows indicate inclining of the magnetization by small angle up and down against the circle plane, respectively. The dashed line in (a) indicates the BC.

The light and black magnetic contrasts in the periphery of the circle are aroused because of up- and down-inclination of the magnetization by a small angle out of the circle plane. The easy axes of magnetization in this case are parallel or perpendicular to the BC, which is in agreement with the results of the study of the film magnetoresistance (note that these microstructures have been fabricated at an angle of 45° to the BC and an X-axis of the MFM scans makes 45° angle against to the BC). As a result of the micromagnetic calculation, the interpretation of the magnetic structure of the circle was perfectly confirmed (Figure 10b).

The results of the experimental study of the FCA microstructures by the MFM supported by the micromagnetic calculation allowed us to find the spatial distribution of magnetization in microstructures, to reveal the appearance of uniaxial and biaxial magnetic anisotropies, which manifests itself in their depending on the growth conditions and annealing of the films, and to find the direction of the easy axes of magnetization with respect to the BC. The results of MFM studies are consistent with the results of film magnetoresistance data.

4. Conclusion

Fe_2CoAl films were grown for the first time on the R-plane sapphire with and without the W seed layer and exhibited close dependences. Films grown on seed layer have demonstrated higher quality under optimal growth. Non-monotonic temperature dependences of morphological and magnetic properties were found. At low growth temperatures $T_g < 50\,^{\circ}C$, the films have $S_q = 0.3$–0.6 nm, $L_c = 40$–70 nm, and close to biaxial anisotropy with $H_c \approx 30$ Oe and $\Delta H_c \approx 100$ Oe. At growth temperatures $50 < T_g < 170\,^{\circ}C$, there was a fast increase by almost an order of H_c and ΔH_c till 250 Oe and about 600 Oe, respectively. This caused, as assumed, the growth of some disordered phase, in which the biaxial magnetic anisotropy was presented and the easy axes of

magnetization were parallel/perpendicular to the BC. S_q = 0.3–0.7 nm and L_c = 65–100 nm. At growth temperatures 170–400 °C, a more ordered phase appeared. At the beginning of this temperature range, the magnetic anisotropy became uniaxial, with the easy axis of magnetization forming an angle of 45° to the BC. At optimal growth temperatures $T_g \approx 300$ °C, the uniaxial state remained, but the easy axis of magnetization became parallel to the BC; the H_c and ΔH_c decreased sharply down to the values 10 Oe for the films grown on seed layer. S_q and L_c reached minimum values 0.2 nm and 30–60 nm, respectively. Further increase of $T_g > 400$ °C led to gradual degradation of the ordered phase with an increase in S_q, L_c, H_c, and ΔH_c. A biaxial magnetic anisotropy appeared. Annealing at temperatures 400–600 °C of the films grown under the optimal conditions improved their magnetic properties – H_c, ΔH_c, and $(\Delta R_{tran})/|(\Delta R_{long})|$ became smaller. Annealing at higher temperature led to degradation of the ordered phase and the appearance of biaxial magnetic anisotropy. The obtained results motivate further studies of the films structural properties with controlling conductive electrons spin polarization degree.

Acknowledgements

The project is jointly supported by DST & RFBR (under Indo-Russian joint project). Dr. D. P. Rai acknowledges Department of Science and Technology (DST) New Delhi, Govt. of India vide Lett. No. INT/RUS/RFBR/P-264. Other authors acknowledge Russian Foundation for Basic Research, grant RFBR 17-57-45024.

References

[1] R. A. De Groot, F. M. Mueller, P. G. v. Engen, and K. H. J. Buschow, New class of materials: Half-metallic ferromagnets, *Phys. Rev. Lett.* **50**(25), 2024 (1983). DOI: 10.1103/PhysRevLett.50.2024.

[2] A. Hirohata, W. Frost, M. Samiepour, and J. н. Kim, Perpendicular magnetic anisotropy in Heusler alloy films and their magnetoresistive junctions, *Materials.* **11**(1), 105 (2018). DOI: 10.3390/ma11010105.

[3] K. Gross *et al.*, Magnetic domain patterns in Co_2MnGe Heusler nanostripes, Phys. *Rev. B.* **84**, 054456 (2011).

[4] Y. I. Matsushita *et al.*, Large magnetocrystalline anisotropy in tetragonally distorted Heuslers: a systematic study, *J. Phys. D: Appl. Phys.* **50**(9), 095002 (2017). DOI: 10.1088/1361-6463/aa5441.

[5] W. H. Wang *et al.*, Spin polarization of single-crystalline Co_2MnSi films grown by PLD on GaAs (001), *J. Magn. Magn. Mater.* **286**, 336 (2005). DOI: 10.1016/j.jmmm.2004.09.089.

[6] H. Schneider *et al.*, Structural, magnetic and transport properties of Co_2FeSi Heusler films, *J. Phys. D: Appl. Phys.* **40**(6), 1548 (2007). DOI: 10.1088/0022-3727/40/6/S06.

[7] G. M. Mikhailov, I. V. Malikov, A. V. Chernykh, and V. T. Petrashov, The effect of growth temperature on electrical conductivity and on the structure of thin refractory metal films, grown by laser ablation deposition, *Thin Solid Films.* **293**(1–2), 315 (1997). DOI: 10.1016/S0040-6090(96)08953-5.

[8] I. V. Malikov, L. A. Fomin, and V. Yu, Vinnichenko, and G. M. Mikhailov, Epitaxial Fe films and structures, Proc. SPIE **7025**, 70250U (2008).

[9] G. M. Mikhailov *et al.*, Complementary analysis of epitaxial Fe (001) films with improved electronic and magnetic transport properties, *Solid State Phenom.* **168–169**, 300 (2010). DOI: 10.4028/www.scientific.net/SSP.168-169.300.

[10] M. Gillessen, and R. Dronskowski, A combinatorial study of inverse Heusler alloys by first-principles computational methods, *J. Comput. Chem.* **31**, 612 (2010). DOI: 10.1002/jcc.21358.

[11] D. Comtesse, Dissertation, First-principles investigation of magnetic and electronic transport properties of transition metal alloys, Universitat Duisburg-Essen (2014).

[12] V. Jain *et al.*, Comparative study of the structural and magnetic properties of bulk and nano-sized Fe_2CoAl, AIP Conf. Proc. **1536**, 935–936 (2013).

[13] E. S. Popiel, W. Zarek, and M. Tuszyński, Mossbauer study of the Heusler-type Fe_2MAl compounds for M = V, Cr, Fe, Co, Ni, *Nucleonika.* **49**, S49 (2004).

[14] G. M. Mikhailov, A. V. Chernykh, and V. T. Petrashov, Electrical properties of epitaxial tungsten films grown by laser ablation deposition, *J. Appl. Phys.* **80**(2), 948 (1996). DOI: 10.1063/1.362906.

[15] L. A. Fomin, V. Yu. Vinnichenko, I. V. Malikov, and G. M. Mikhailov, Micromagnetic states in Fe(001) rectangular epitaxial microstructures: The effect of magnetic anisotropy and aspect ratio, *J. Magn. Magn. Mater.* **330**, 6 (2013). DOI: 10.1016/j.jmmm.2012.08.001.

[16] G. M. Mikhailov, A. V. Chernykh, and L. A. Fomin, Application of magnetic force microscopy for investigation of epitaxial ferro- and antiferromagnetic structures, *Materials.* **10**(10), 1156 (2017). DOI: 10.3390/ma10101156.

[17] http://math.nist.gov/oommf

[18] L. A. Fomin *et al.*, Switching the direction of circumferential magnetization of square epitaxial Fe (001) microstructures by spin-polarized current, *Russ. Microelectron.* **42**(5), 309 (2013)., DOI: 10.1134/S1063739713050041.

[19] L. Siakeng, G. M. Mikhailov, and D. P. Rai, Electronic, elastic and X-ray spectroscopic properties of direct and inverse full Heusler compounds Co_2FeAl and Fe_2CoAl, promising materials for spintronic applications: a DFT + U approach, *J. Mater. Chem. C.* **6**(38), 10341 (2018). DOI: 10.1039/C8TC02530D.